Proceedings of the Korean Nuclear Society Autumn Meeting
Suwon, Korea, October 2001

Diode Laser-induced Glow Discharge Optogalvanic Spectroscopy for the Wavelength Calibration in the Near Infrared Wavelength Region

E. C. Jung and Cheol-Jung Kim
Korea Atomic Energy Research Institute
P. O. Box 105, Yusong, Taejon 305-600, Korea

Abstract

Optogalvanic spectra have been recorded by axially irradiating hollow uranium cathode glow discharge with a single-mode diode laser. Fifty uranium transitions have been tabulated with optogalvanic signal magnitudes in the 662-680, 774-792, 834-862 nm region for wavelength calibration. Atomic excitation temperature has been determined by the measured signal magnitudes.

1. Introduction

When a gas discharge is irradiated with a laser light tuned to the resonance frequency of an atomic transition, the optogalvanic (OG) effect, the change of the discharge impedance, will result from the change in atomic population between the states [1]. Because of the simple experimental setup and highly sensitive characteristics, the most common application of OG spectroscopy to date has been the recording of atomic spectra [2]. Precise wavelength determinations of atomic transitions are possible by OG detection and, conversely, the OG spectra with accurately known wavelengths can provide a convenient means of calibrating the wavelengths of tunable lasers.

In the past, many OG lines have been observed in fill gases like neon [3-5] and argon [6-8], in species sputtered from hollow cathodes like uranium [9-11], thorium [11] and iron [12]. But most OG atlases are limited to the visible and UV

wavelength regions. Now tunable diode lasers are being widely used in the field of atomic and molecular spectroscopy. Thus it is of interest to record atomic lines having good OG signals in the near-IR wavelength region for either wavelength calibration or frequency stabilization of diode lasers.

In this paper, we are reporting the OG spectra of sputtered uranium in a commercial hollow cathode glow discharge tube. The choice of uranium cathode is particularly useful for our purpose of wavelength calibration because this element gives very dense spectral lines and the wave numbers of the transitions have been known to an accuracy of ± 0.002 cm^{-1} [13]. Fifty uranium transitions in the wavelength region of 662-680, 774-792, 834-862 nm are tabulated with the OG signal magnitudes in our work. Moreover, the atomic excitation temperature in a discharge has been determined by the measured OG signal magnitudes with the aid of known oscillator strengths of the transitions.

2. Experiment

The experimental setup is shown schematically in Fig. 1. Single-mode radiation (a line-width of about 1 MHz/sec) was provided by an external cavity diode laser (New Focus Inc., model 6200 controller with 6202, 6224, 6226 laser heads). An achromatic anarmophic prism pair (New Focus Inc., model 5411) was used for transforming the elliptical shape of a laser beam into a circular one. The diameter of the laser beam was adjusted by iris diaphragms of 1 mm diameter. The laser beam at the constant power of 0.6 mW with an error of less than 0.01 mW was illuminated into a see-through type commercial uranium hollow cathode glow discharge tube filled with Ar buffer gas (Cathodeon Inc., model 3QQAY/U, buffer gas pressure of about 6 torr). The electrodes were connected to a stabilized dc power supply (Bertan Associate Inc., model 105-01R) with a voltage of 275 V at a current of 30 mA. A current limiting load resistor of 10 kΩ was placed in series with the discharge tube and a source of constant dc voltage. An increase in voltage across the discharge tube upon laser irradiation is accompanied by a corresponding decrease in discharge current. The OG signal was detected with a lock-in amplifier (EG&G, model 5210) by blocking the dc voltage using a coupling capacitor of 0.01 μF. Absorption of the laser beam intensity

was monitored by a photo-diode (Newport, model 818-BB-20). A small part of the laser beam was sent to a wavemeter (Burleigh., model WA-4500) or confocal Fabry-Perot etalon (Tec Optics, model SA-300) having a free spectral range of 0.3 GHz.

3. Results and Discussion

Typical OG spectra are shown in Fig. 2. The measurement can be performed within a few seconds. The magnitudes of the OG signals, I_{OG}, resulting from 0.6 mW irradiation are listed in Table 1, 2 and 3 for selected fifty transitions. Many other transition lines can be measured in these wavelength regions [13], but all of unlisted lines are very weak and no special effort was made to detect them. Also listed in each Table are oscillator strengths (usually reported as gf values, where g is the statistical weight of the lower state and f is the oscillator strength of the transition) and lower energy levels for those transitions. These spectroscopic parameters have been taken from the work of Palmer et al. [13]. The relative values of gf have estimated errors of about 8%. Although transitions from energy levels as high as 16041 cm^{-1} were observed, the large majority of the measured transitions arise from low odd parity levels placed below 10,000 cm^{-1}.

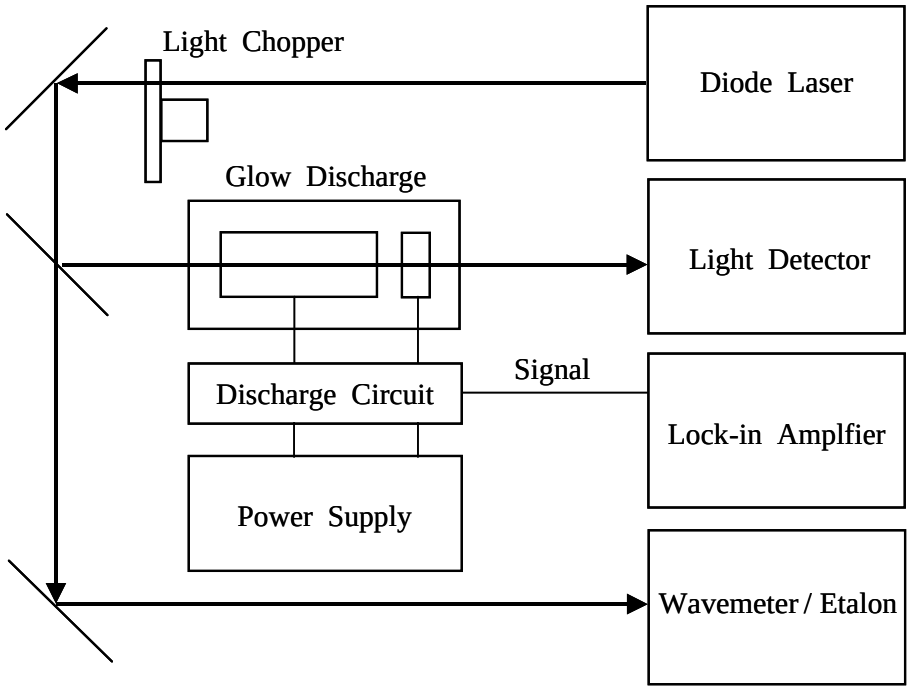

Fig. 1 Experimental setup for optogalvanic spectroscopy.

Closer inspection of the last columns in each table shows that there is an apparent trend towards decreasing $I_{OG}/\lambda gf$ as the energy of the lower state in column 2 increases. As was first observed for uranium [9], the OG signal magnitude for the sputtered species in the discharge is proportional to the cross section for absorption of light multiplied by the atomic concentration of the lower level, [A], in the transition:

$$I_{OG} \propto \lambda_{AB} \cdot f_{AB} \cdot [A]. \tag{1}$$

On the assumption of a local thermodynamic equilibrium in a plasma, the atomic population has a Boltzmann distribution:

$$[A] \propto g_A \cdot e^{\frac{-E_A}{kT_{EX}}}, \tag{2}$$

where g_A and E_A are the statistical weight and energy level of the lower state, respectively, k is the Boltzmann constant, T_{EX} is an atomic excitation temperature. Then

$$\ln \frac{I_{OG}}{\lambda_{AB} \cdot g_A \cdot f_{AB}} = C - \frac{E_A}{kT_{EX}}, \tag{3}$$

where C is the constant containing units and scale factor. Plotting left term in Eq. (3) versus E_A (often called a "Boltzmann plot") gives a line with a slope equal to $(-1/kT_{EX})$.

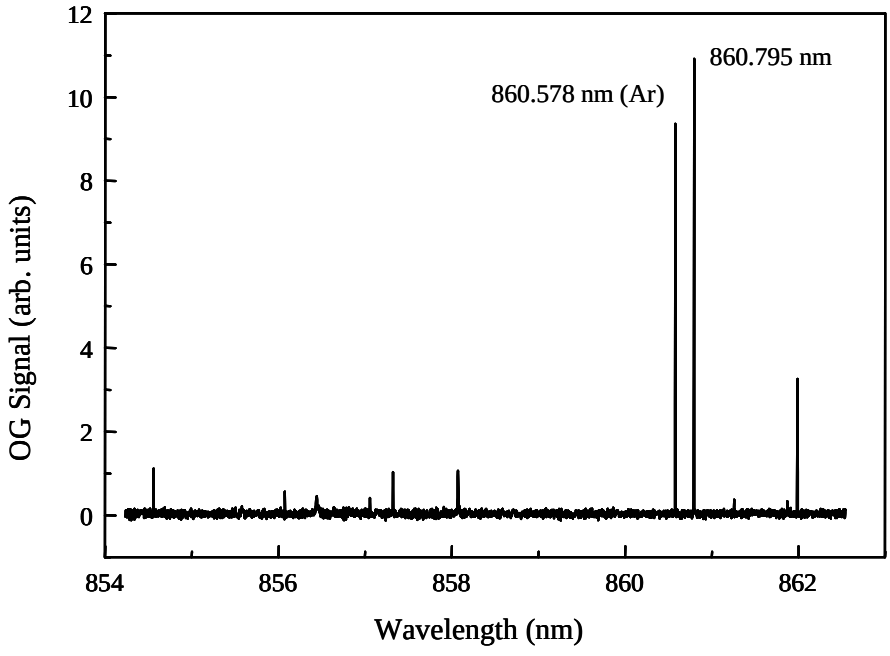

Fig. 2. Typical optogalvanic spectra.

Table 1. Optogalvanic spectra of uranium for the wavelength calibration of diode laser having center wavelength of 670 nm.

Wavelength (nm)	Lower energy level (cm^{-1})	gf	I_{OG} (mV)	I_{OG} / λgf
662.52957	5762	0.0315	0.100	47988
664.77929	3801	0.0108	0.058	80946
665.68188	620	0.0065	0.130	302696
668.33848	3801	0.0333	0.200	89921
672.79721	5762	0.0251	0.097	45654
673.68046	0	0.0068	0.220	478554
674.13641	6249	0.1012	0.243	35621
676.86418	7864	0.0414	0.061	21779
678.25998	5988	0.0230	0.063	40463
678.28570	4453	0.0172	0.071	60757
679.03029	7646	0.1295	0.168	19120

Table 2. Optogalvanic spectra of uranium for the wavelength calibration of diode laser having center wavelength of 780 nm.

Wavelength (nm)	Lower energy level (cm^{-1})	gf	I_{OG} (mV)	I_{OG} / λgf
774.81903	16041	0.6831	0.055	1039
775.98806	7646	0.0473	0.105	28611
776.18507	7006	0.0608	0.154	32648
778.41587	620	0.0903	2.210	314514
781.63278	13128	0.2847	0.060	2696
783.57385	5991	0.0193	0.088	58185
784.47200	16041	0.5382	0.041	971
786.87396	7864	0.0313	0.067	27184
786.87878	3801	0.0281	0.260	117705
787.53929	11308	0.2608	0.140	6816
788.19441	6249	0.4770	1.140	30323
789.60320	13128	0.1472	0.035	3011
790.04339	4276	0.0220	0.160	92029
790.42933	8119	0.0638	0.099	19640
790.79822	7006	0.0206	0.075	45997
791.88150	4276	0.0280	0.203	91683

Table 3. Optogalvanic spectra of uranium for the wavelength calibration of diode laser having center wavelength of 850 nm.

Wavelength (nm)	Lower energy level (cm^{-1})	gf	I_{OG} (mV)	I_{OG} / λgf
834.67576	5991	0.0545	0.202	44422
835.70605	3868	0.0135	0.108	96024
838.18709	7006	0.1308	0.310	28284
838.72018	4276	0.0205	0.153	88857
838.75677	7864	0.0234	0.057	29010
838.91689	5991	0.0504	0.207	48973
839.92437	5991	0.0191	0.106	66015
842.67471	3868	0.0065	0.060	109564
844.12048	7646	0.1426	0.275	22840
844.53826	3801	0.1322	1.060	94933
845.00312	3801	0.1000	0.820	97079
849.60939	8119	0.1449	0.173	14052
850.45510	11457	0.2753	0.108	4613
854.01846	5762	0.0937	0.411	51373
854.23313	10255	0.1050	0.085	9473
855.73309	10686	0.1866	0.123	7704
856.69409	10289	0.0735	0.059	9376
856.77189	4453	0.0264	0.189	83701
857.05168	8119	0.2634	0.368	16301
857.46051	6249	0.0572	0.182	37137
860.79503	0	0.1240	4.380	410448
861.27765	5762	0.0196	0.107	63416
861.84599	5762	0.0168	0.082	56599

Fig. 3 shows the Boltzmann plot. The fitted solid line by least-squares regression shows a linear-correlation coefficient of 0.993. The slope of this line yields an atomic excitation temperature of 3812 ± 68 K. The estimated uncertainty of temperature was derived from the standard deviation error of the slope in the least-squares program.

Regardless of a good linear-correlation coefficient and standard deviation uncertainty in Fig. 3, we have to note that the linear dependence of the OG signal magnitude on the *gf* value in Eq. (1) and the assumption of local thermodynamic equilibrium in Eq. (2) must be verified as pointed in Ref. 14 at our discharge condition. To convince the former relationship the simultaneous detection of both OG and the absorption signals has been performed because the absorption coefficient is directly related to the oscillator strength in classical absorption spectroscopy.

In Fig. 4 the OG line profile represented by a dotted line is compared with the absorption one represented by a solid line at 860.79503 nm. In this measurement frequency detuning of the diode laser was made by the modulation of laser cavity length with a modulation frequency of 100 Hz. Both signals were monitored by a digital storage oscilloscope (Lecroy Inc., model 9450) and normalized to a common peak value for a better comparison. The bottom trace shows the interference fringe of confocal Fabry-Perot etalon for the laser frequency marker. We observed that the OG line profiles agreed with the absorption line profiles within the discharge current ranging from 10 to 70 mA.

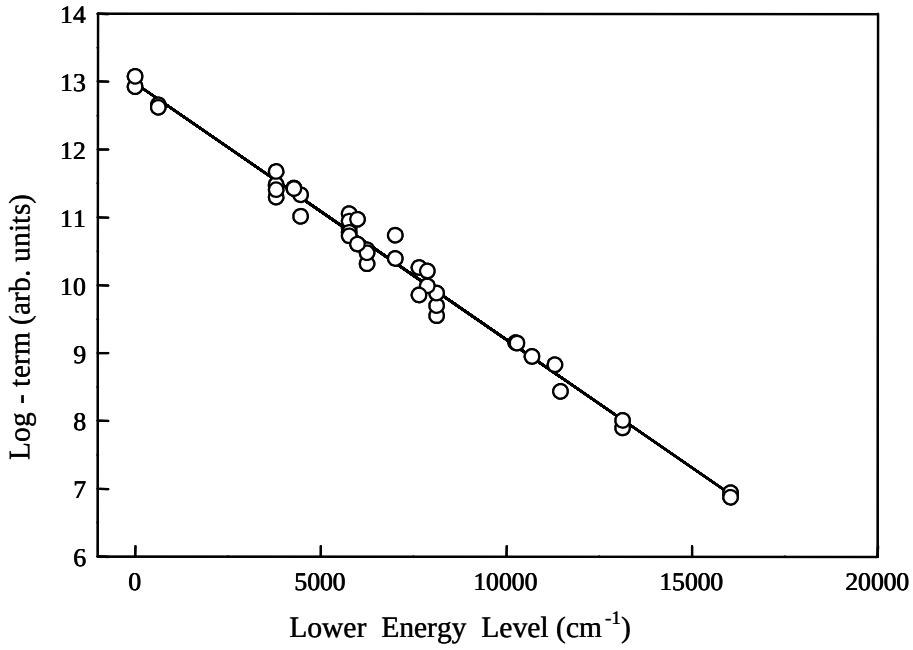

Fig. 3. Boltzmann plot by Eq. (3) at the discharge current of 30 mA. Data in Table 1, 2 and 3. The slope of the line yields an atomic excitation temperature of 3812 ± 68 K with a linear correlation coefficient of 0.993.

Fig. 5 shows the dependence of both OG signal magnitude and peak absorption on the input laser power at the discharge current of 50 mA. The OG signal magnitude represented by solid line was normalized to an absorbed laser power. The good agreement between both signals was also observed within the discharge current ranging from 10 to 70 mA. It is reasonable to conclude that a linear relationship exists between the OG signal magnitudes and the *gf* values from the results of Fig. 4 and 5.

The validity of the assumption of a Boltzmann distribution, which requires local thermodynamic equilibrium, as described in Eq. (2) and (3) has been confirmed by the independent emission measurement. For conventional emission spectroscopy, plotting

$$\ln \frac{I_{EMI} \cdot \lambda_{BA}}{g_B \cdot A_{BA}} = C - \frac{E_B}{kT_{EX}} \tag{4}$$

gives a line with a slope equal to ($-1/kT_{EX}$) under the Boltzmann distribution [15,16].

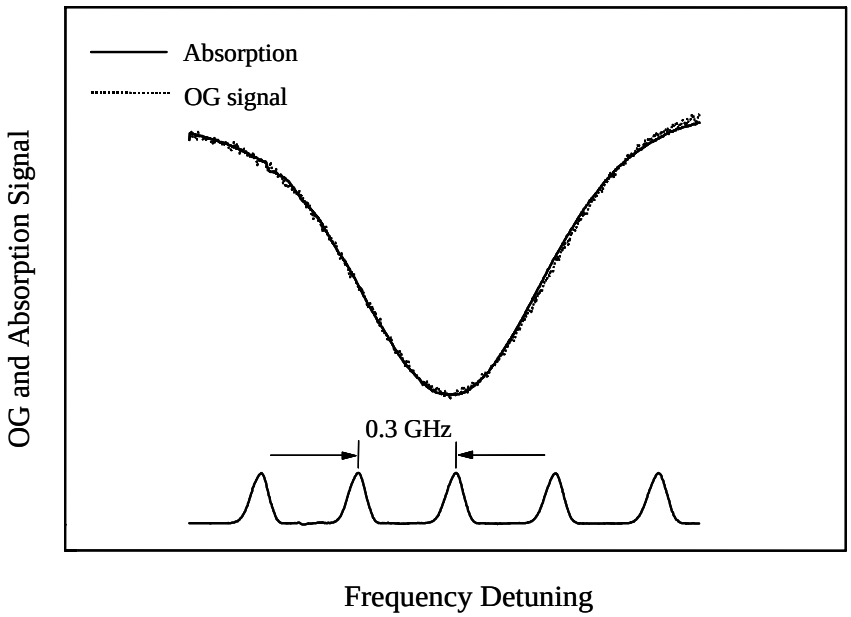

Fig. 4. Comparison of optogalvanic (dashed) and absorption (solid line) profiles of the transition at 860.79503 nm (0-11613.9771 cm^{-1}). Laser power of 5 mW, discharge current of 50 mA. Peak absorption is about 15%. Optogalvanic signal is normalized to the peak absorption. Bottom trace is the frequency marker by confocal Fabry-Perot etalon.

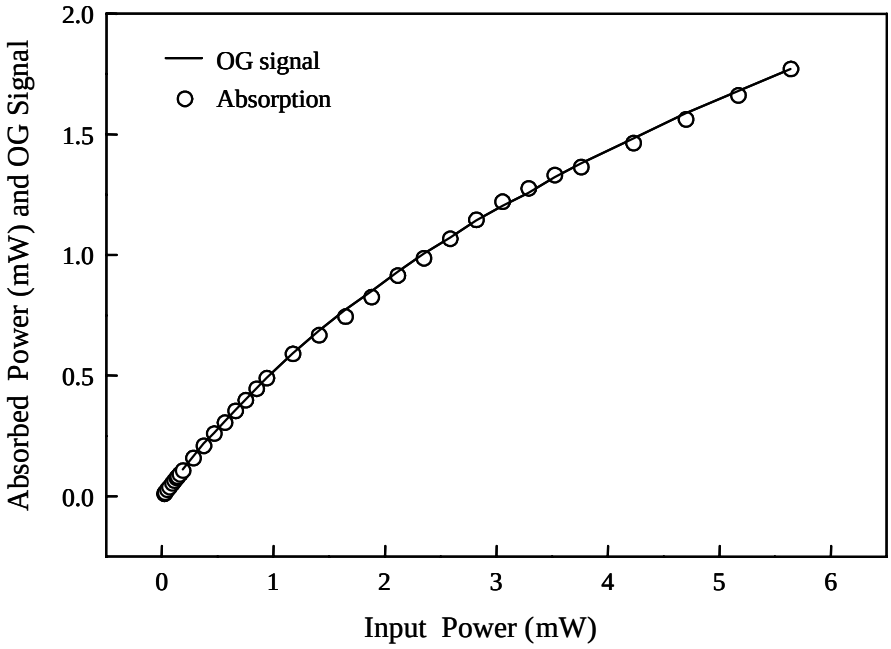

Fig. 5. The dependence of the optogalvanic signal (solid line) and absorbed laser power (circles) at the peak upon the input laser power. The optogalvanic signal is normalized to the absorbed laser power.

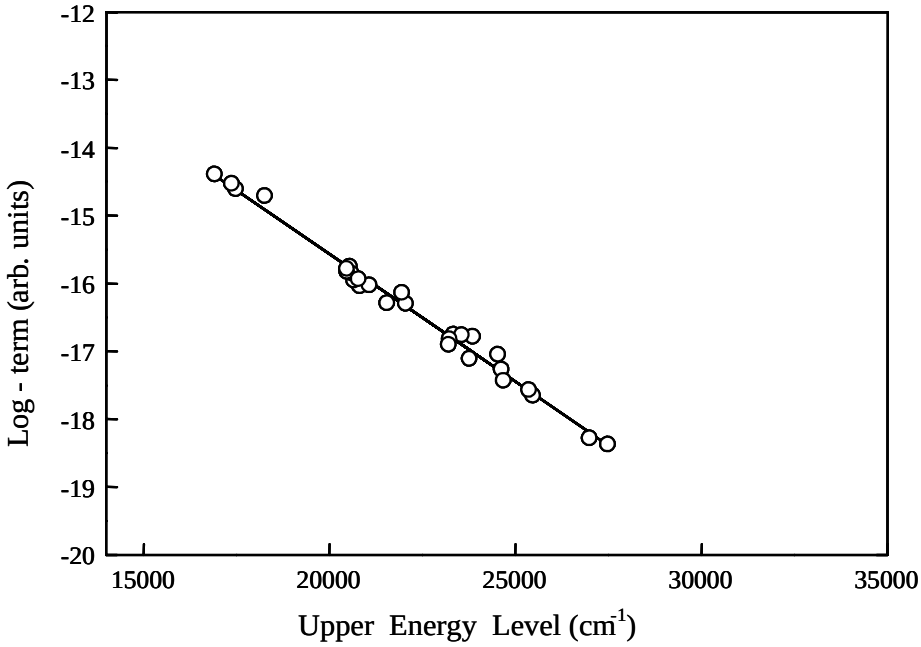

Fig. 6. Boltzmann plot by Eq. (4) at the discharge current of 30 mA. The slope of the line yields an excitation temperature of 3828 ± 82 K with a correlation coefficient of 0.994. These values are nearly equivalent to the values as appeared in Fig. 3.

In this equation, I_{EMI} is a emission intensity, g_B and E_B are the statistical weight and energy level of the upper state, respectively, A_{BA} is the transition probability of the transition. We measured twenty eight uranium emission lines within the wavelength ranging from 566 to 607 nm at the discharge current of 30 mA. The detailed experimental setup and spectroscopic information of these lines were published elsewhere [17]. The Boltzmann plot of emission lines is shown in Fig. 6. The slope of solid line yields an excitation temperature of 3828 ± 82 K with a correlation coefficient of 0.994. These values are almost comparable to the result obtained by OG measurement in Fig. 3.

4. Conclusion

In summary, we tabulated fifty uranium OG lines which are useful for the wavelength calibrations of commercially available diode lasers having the center wavelength of 670, 780 and 850 nm, respectively. In our discharge conditions, buffer gas pressure of about a few torr and discharge current of a few tens mA, the response of the plasma represented by OG effect is closely linked to an absorption phenomenon. Under the Boltzmann distribution of sputtered atomic species, the excitation temperature has been determined.

References

[1] R. B. Green, R. A. Keller, G. G. Luther, P. K. Schenck and J. C. Travis, Appl. Phys. Lett. 29, 727 (1976).

[2] B. Barbieri, N. Beverini and A. Sasso, Rev. Mod. Phys. 62, 603 (1990).

[3] E. F. Zalewski, R. A. Keller and R. Engleman, Jr., J. Chem. Phys. 70, 1015 (1979).

[4] J. R. Nestor, Appl. Opt. 21, 4154 (1982).

[5] B. R. Reddy and P. Venkateswarlu, Opt. Commun. 85, 491 (1991).

[6] M. Su, S. R. Ortiz and D. L. Monts, Opt. Commun. 61, 257 (1987).

[7] B. R. Reddy, P. Venkateswarlu and M. C. George, Opt. Commun. 75, 267 (1990).

[8] M. Hippler and J. Pfab, Opt. Commun. 97, 347 (1993).

[9] R. A. Keller, R. Engleman, Jr., and E. F. Zalewski, J. Opt. Soc. Am., 69, 738 (1979).

[10] N. J. Dovichi, D. S. Moore and R. A. Keller, Appl. Opt. 21, 1468 (1982).

[11] C. J. Sansonetti and K. H. Weber, J. Opt. Soc. Am. B 1, 361 (1984).

[12] F. Babin, P. Camus, J. M. Gagné, P. Pillet and J. Boulmer, Opt. Lett. 12, 468 (1987).

[13] B. A. Palmer, R. A. Keller and R. Engleman, Jr., *An Atlas of Uranium Intensities in A Hollow Cathode Discharge*, Los Alamos National Laboratory Informal Report, LA-8251-MS, UC-34a (1980).

[14] H. A. Bachor, P. J. Manson and R. J. Sandeman, Opt. Commun. 43, 337 (1982).

[15] G. Yu. Grigorev, A. V. Eletskii, V. D. Klimov, O. A. Kushlyanskii, M. Ya. Minakov and A. M. Mosolov, Opt. Spectrosc. 69, 22 (1990).

[16] R. A. Keller, B. E. Warner, E. F. Zalewski, P. Dyer, R. Engleman, Jr., and B. A. Palmer, J. Phys. (Paris) C7-44, 23 (1983).

[17] E. C. Jung, Kyuseok Song, Hyungki Cha, and Jongmin Lee, Sectrosc. Lett. 31, 1151 (1998).